COUPLING MULTIPLE STIFF PROCESSES IN REACTIVE FLOW SIMULATIONS

Jay P. Boris, Elaine S. Oran, Gopal Patnaik
Laboratory for Computational Physics and Fluid Dynamics
U.S. Naval Research Laboratory, Code 6400
Washington D.C. 20375

This paper describes a new method, Compensated Operator Splitting (COS), for coupling several distinct, mathematically stiff, reactive flow processes into a dynamic simulation model. Operator splitting (also called process splitting or or timestep splitting) is the simplest way to build numerical models containing a number of different reactive-flow processes and allows use of optimal algorithms for each of the processes individually [1]. However, explicit operator-splitting performs poorly in situations where two or more of the processes are "stiff" and thus require unacceptably small timesteps. Global-implicit coupling can in principle be used for these cases, but the computational cost becomes prohibitive, the programming is often complex, there are serious algorithmic restrictions, and the accuracy can be quite low. Here we describe how operator splitting can be extended to a broad class of problems having interacting stiff processes. This is particularly important for solving the highly exothermic reactive flows appearing in combustion systems.

There are two situations where stiffness in more than one process makes the problem difficult to solve. These are when: 1) Rapid transients arise because one or more of the stiff processes are far from equilibrum, and 2) Competing stiff processes are operating close to their common, dynamic equilibrum. Rapid transients, with some of the processes far from equilibrum, need to be solved on the appropriate short time scales to obtain accurate answers. The saving grace is that the situation *is* transient. The second type of stiffness concerns relatively slowly-varying systems whose evolution is dynamic balance of several stiff processes. When this type of stiffness exists, the solution is difficult and expensive because the integration must be carried out for a relatively long time.

We use a model problem of a laser-driven reactive flow to illustrate COS. A flowing gas intersects the beam of a high-intensity laser that heats a small volume. This generates radicals and drives further chemical reactions. In the frame of reference of a fluid element moving into the laser spot, the fluid is being rapidly heated and the system may be far from chemical and thermal equilibrium. Stiff chemical reactions occur in and near this deposition volume. Because the depostion region is narrow with small spatial scales and large gradients, thermal conduction and molecular diffusion of the newly created radicals are also stiff in this region. The fluid dynamics is stiff because the sound speed is much greater than the flow speed. Despite the strong dynamics of the reactive flow in the frame of the moving fluid, this problem has a steady-state solution in the laboratory frame when the laser intensity is constant. After the initial rapid transients, we expect an expanding, cooling wake with no time variation behind the laser spot. The stiff processes find a joint equilibrum in which thermal conduction, molecular diffusion, convection, and the thermally-driven chemical reactions take energy and radicals away from the hot region as the laser adds energy and creates radicals.

In this paper we solve two scalar equations, one for a radical species $\rho(r,z,t)$ and another for the temperature $T(r,z,t)$,

$$\frac{\partial \rho\,(r,z,t)}{\partial t} = \frac{1}{r}\frac{\partial}{\partial r}\left(rD\frac{\partial \rho}{\partial r}\right) + \frac{\partial}{\partial z}\left(D\frac{\partial \rho}{\partial z}\right) + G_L^{\rho}(r,z,t) + \Gamma(T)\ (\rho_{eq}(T) - \rho(r,z,t)\,) - V_z\frac{\partial \rho}{\partial z}\,, \tag{1}$$

$$\begin{aligned}\frac{\partial T\,(r,z,t)}{\partial t} &= \frac{1}{r}\frac{\partial}{\partial r}\left(rK\frac{\partial T}{\partial r}\right) + \frac{\partial}{\partial z}\left(K\frac{\partial T}{\partial z}\right) + G_L^{T}(r,z,t) \\ &\quad - \frac{\Delta T}{\Delta \rho}\,\Gamma(T)\ (\rho_{eq}(T) - \rho(r,z,t)\,) - V_z\frac{\partial T}{\partial z}\ .\end{aligned} \tag{2}$$

The operator-split structure of Eqs. (1) and (2) for this problem, can be written more generally as

$$\frac{\partial \boldsymbol{\rho}}{\partial t} \equiv G_R(\boldsymbol{\rho}) + G_Z(\boldsymbol{\rho}) + G_L(r,z,t) + G_C(\boldsymbol{\rho}) + G_F(\boldsymbol{\rho})\ , \tag{3}$$

where the subscript R designates radial diffusion, Z axial diffusion, L laser deposition, C chemical reactions, and F fluid dynamics. The laser source components ${G_L}^{\rho}(r,z,t)$ and ${G_L}^{T}(r,z,t)$ are Gaussians. The

temperature-dependent chemical reaction rate $\Gamma(T)$ specifies the rate at which the radical density approaches the equilibrium radical density $\rho_{eq}(T)$, which increases exponentially with temperature. The molecular diffusion coefficient D and the thermal conduction K are constants taken to be large enough that the radial and axial diffusion would be unstable if an explicit algorithm were used. Diffusion is broken into separate stiff operators in the radial and axial directions. The global timestep $\Delta t_g = \Delta z / V_z$ is determined by the flow velocity, V_z, and the spacing of the grid, Δz. The reaction and diffusion stiffness factors vary from unity to a factor of about forty depending on the spatial resolution.

Figure 1 shows the evolution of this example system with five physical processes in the phase plane of the radical density and fluid temperature. The arrows indicate the vector contributions of the five processes schematically during each of several timesteps. The sum of these vector contributions for ρ and T follows a trajectory in the (ρ, T) plane indicated in the figure by the sequence of discrete times t_0, t_1, t_2, and t_3. The separation of these points shows how much the solution actually changes each timestep. The three loops of vectors show how the contributions of the individual processes nearly cancel. In steady state, each loop would close perfectly since the solution does not change. This has generally been considered to be a situation for which operator splitting (also called timestep splitting or process splitting) does not work, and where global implicit coupling must be used.

The basic concept of COS is to integrate each process separately using a current, accurate estimate to compensate the missing contributions of all the other processes. Let $G_p(\boldsymbol{\rho})$ represent one physical process or a single component of the direction-split representation of a stiff multidimensional process. Define the "minus p" operator $G_{mp}(\boldsymbol{\rho})$ as the sum of all processes minus process p,

$$G_{mp}(\boldsymbol{\rho}) \equiv \sum_{k=1,\, k\neq p}^{M} G_k(\boldsymbol{\rho}) \ . \tag{4}$$

Each process in the global timestep Δt_g is then evaluated separately using

$$\left.\frac{\partial \boldsymbol{\rho}}{\partial t}\right|^{p} = G_p(\boldsymbol{\rho}) + G_{mp}(\boldsymbol{\rho}) \ . \tag{5}$$

The substep integrations are performed sequentially to evaluate the effects of each process $G_p(\boldsymbol{\rho})$ on the system variables. It is important to use the most updated source each time the minus p operator is used. The two requirements on $G_{mp}(\boldsymbol{\rho})$ are that it should: (1) incorporate the most recent approximations to the changes in $\boldsymbol{\rho}$ due to various processes, and (2) permit evaluation before actually updating the physical variables. At every substep of the procedure, it is crucial to enforce the near cancellation of terms that makes the problem stiff. In Figure 1, this means that the individual processes are *not actually evaluated* at the ends of the arrows signifying the composite change associated with all of the previous processes. Instead, the processes are always compensated, so the physical variables used in intermediate evaluations are close to the final values at the end of the timestep.

Figure 2 shows the power of COS, in this case applied to the laser problem. Figures 2a and 2b show grey-scale contours of ρ and T (respectively) for a case with constant laser intensity. Figures 2c and 2d show the analogous solutions at one time for a sinusoidally oscillating laser intensity. Each figure compares the solution for two different grid resolutions. On the left is the solution for a fine computational grid and on the right is the numerical solution at the same time and parameters for a grid ten times coarser. The individual cells can be seen in the coarse computations because no interpolation is used to smooth the solutions.

Parameters for the computations are related to the stiffness factors for the chemistry and diffusion terms at different resolutions. These factors differ between the temperature and the density because different thermal conduction and molecular diffusion coefficients were used. They also differ in the two directions for both diffusion terms because the radial cells are half the size of the axial cells. The chemistry becomes less stiff as the resolution is improved because the global timestep decreases with increased resolution. The diffusion terms, however, become stiffer as the resolution increases because the cell size appears quadratically in the demoninator of the timestep needed for stability. In both the steady-state and time-dependent problems, the solutions are quantitatively similar despite the factor of ten difference in spatial resolution. At both resolutions, all terms are stiff and some of them are very stiff. Convergence and error estimates will also be discussed.

1. E.S. Oran and J.P. Boris, *Numerical Simulation of Reactive Flow*, 1st Edition: Elsevier, New York, 1987, 2nd Edition: Cambridge, New York, 1999.

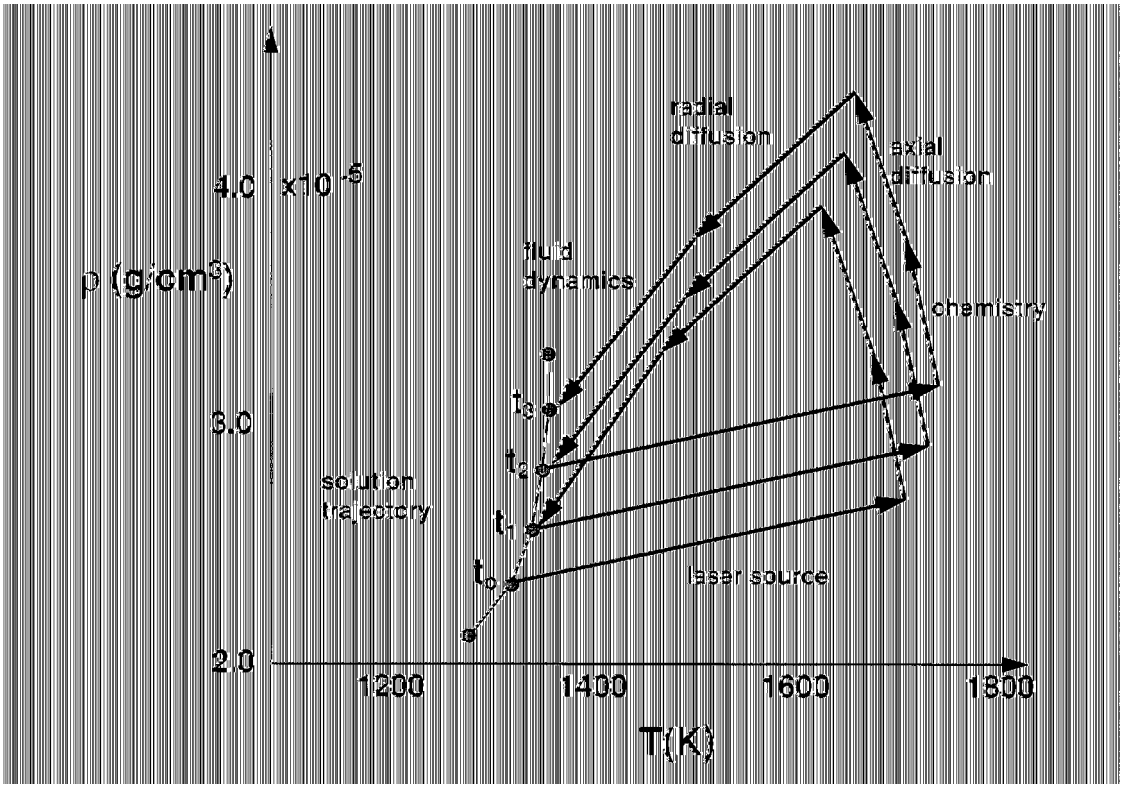

Figure 1. Evolution of a multiply stiff system in the phase plane of a radical density and the fluid temperature. The arrows indicate the vector contributions of the five processes.

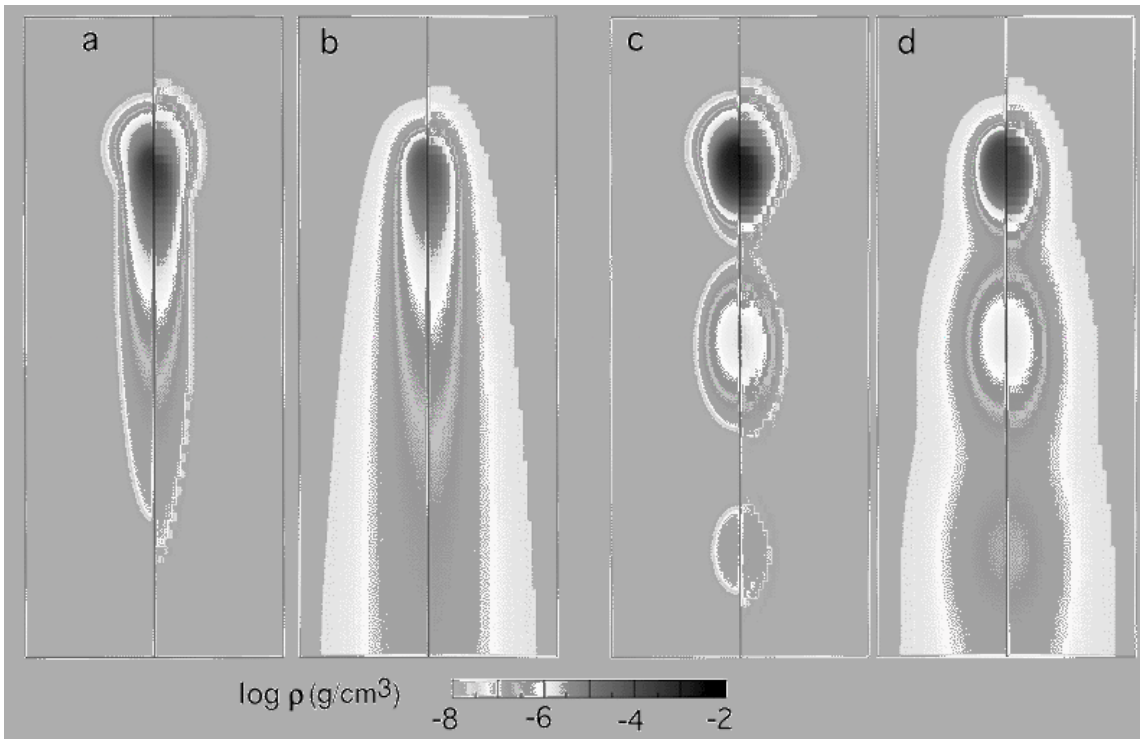

Figure 2. Panels a and b show grey-scale contours of ρ and T respectively for a steady state solution. Panels c and d show the analogous solutions at one time for a sinusoidally oscillating laser intensity. Each panel compares two different grid resolutions; coarse grid cells are visible on the right.